Materials Advances

ROYAL SOCIETY OF CHEMISTRY

PAPER

View Article Online
View Journal | View Issue

Cite this: *Mater. Adv.*, 2025, 6, 4483

Effect of the temperature of biomixing on the pH/temperature sensitive controlled drug release of a chitooligosaccharide-based hydrogel†

Mohammad Muhtasim Ittisaf,[a] Md. Rakid-Ul-Haque,[b] Nishat Tabassum,[c] Mehedi Hasan Pritom,[a] Md. Shad Hossain Tanvir,[a] M. Azam Ali[d] and Shoeb Ahmed *[a]

Chitooligosaccharide (COS)–carboxymethyl cellulose (CMC)–polyethylene glycol diacrylate (PEGDA) hydrogel was fabricated through bio-ink mixing at two different temperatures (4 °C and 30 °C) to investigate its drug release performance in gastric and intestinal fluid conditions. The polyelectrolyte complex was transformed into a hydrogel through UV crosslinking using Irgacure 2959 as the photoinitiator. Vancomycin hydrochloride (COVAN) was loaded into the hydrogel solution by mixing it. Fourier transform infrared spectroscopy (FTIR), scanning electron microscopy (SEM), X-ray diffraction (XRD), differential scanning calorimetry (DSC), and thermogravimetric analysis (TGA) were done to characterize the two different hydrogels with and without the drug. The hydrogels exhibited pH and temperature-responsive swelling behavior. The equilibrium swelling ratio for both the drug-free hydrogels was highest at 6.8 pH and 37 °C, having a value of ~1000%, and the lowest at 1.2 pH at 450–650%. 4°(D)-drug-incorporated hydrogel mixed at 4 °C showed the highest release in intestinal fluid conditions at 37 °C with around 98% of the total drug released after a day. 4°(D) showed higher drug release in a sustained manner at 1.2 pH, 37 °C, but lower drug release at 1.2 pH, 30 °C compared to *N*(D) (drug incorporated regular hydrogel mixed at 30 °C). The drug release data fit into the Korsmeyer–Peppas model, where the *n* value indicated a Fickian drug transport in most cases. 4°(D) showed higher drug release and higher drug incorporation compared to *N*(D) under most conditions. 4°(D) also showed a greater inhibitory effect against Gram-positive bacteria *B. cereus*, lower minimum inhibitory concentration (MIC), and lower minimum bactericidal concentration (MBC) compared to *N*(D). Therefore, altering the temperature of mixing of the hydrogel solution has the potential to improve the drug delivery systems and achieve better therapeutic value. In this case, 4°(D) has potentially greater efficacy than *N*(D) as a bactericide for various Gram-positive bacteria. This study also establishes biomixing temperature as a significant parameter for the future treatment of colonic diseases such as Crohn's disease, ulcerative colitis, *etc.*

Received 17th December 2024,
Accepted 23rd May 2025

DOI: 10.1039/d4ma01261e

rsc.li/materials-advances

1. Introduction

Hydrogels are three-dimensional (3D) porous networks that resemble the extracellular matrix (ECM). Due to its resemblance to the ECM and ability to imbibe or retain large amounts of water, hydrogel is an attractive option for drug delivery systems (DDSs) and cell culture.[1] Based on the differences in toxicity, stimulus responsiveness, and drug encapsulation efficiency, physically crosslinked hydrogels are preferred over chemically crosslinked hydrogels.[2] This reference is due to the free end chains, network defects caused by ionic dipole interaction, or H-bonding in physically crosslinked hydrogels that induce their reversible nature, imperative for high drug release efficiency.[3] Thus, this general class of hydrogel has had success

[a] *Department of Chemical Engineering, Bangladesh University of Engineering and Technology (BUET), Dhaka-1000, Bangladesh. E-mail: mittisaf@che.buet.ac.bd, pritomhasan.bd@gmail.com, shadhossaintanvir473@gmail.com, shoebahmed@che.buet.ac.bd*
[b] *Department of Chemical & Biomolecular Engineering, University of Illinois Urbana-Champaign, Urbana, IL 61801, USA. E-mail: mrhaque2@illinois.edu*
[c] *Department of Chemical Engineering, Massachusetts Institute of Technology, Cambridge, Massachusetts 02139, USA. E-mail: tabassum@mit.edu*
[d] *Centre for Bioengineering & Nanomedicine, Division of Health Sciences, University of Otago, PO Box 56, Dunedin 9054, New Zealand. E-mail: azam.ali@otago.ac.nz*

† Electronic supplementary information (ESI) available. See DOI: https://doi.org/10.1039/d4ma01261e

in the loading of anti-inflammatory drugs such as ketoprofen,[4] diclofenac,[5] ibuprofen,[6] and vancomycin,[7] among others. However, the recent emergence of synthetic polymers such as PLA, PEG, PGA, and their copolymers, PLGA, has led to the union of natural and synthetic polymers, leading to increased mechanical strength of hydrogels while retaining high bioactivity.[8,9] The choice of synthetic or natural polymers within this broad class enables tuning of the properties of the hydrogel, such as biodegradability, which helps venture into a broad area of application. This can be clinical applications such as stem cell encapsulation and release,[10] stem cell therapies,[11] acute laceration treatment,[12] stem cell differentiation,[13] and breast implants in plastic surgery[14] as well as various organs, such as the small intestine, eyes, lungs, kidneys, and skin.[1]

Chitooligosaccharide (COS) is a chitosan derivative with improved aqueous solubility or bioactive properties compared to chitosan. This is mainly due to the lowering of the molecular weight (MW) and degree of polymerization (DP), and altering the degree of deacetylation (DD). COS usually has an MW $<$ 10 kDa and DP $<$ 10, whereas the DD can vary.[15,16] The tuning of MW and DD can help achieve better performance in terms of therapeutic response, drug loading, release, bioaccumulation, biodegradability, targeting precision, and external stimuli-responsive drug delivery for COS.[17] The lowering of the MW has improved performance in alleviating inflammation by acting as a free radical scavenger, scavenging the oxidative and nitrogen species produced in response to inflammation. COS with MW $<$ 5 kDa is effective in this case by increasing the activity of antioxidative enzymes.[18,19] Chitosan-based hydrogels are an attractive choice for the delivery of polar hydrophilic drugs such as vancomycin, as they bind to the negatively charged regions of the mucosal lipid membranes and, by rearranging the junction proteins, create a channel for the effective delivery of the drug.[20] However, at pH levels above 6, the protonation of the chitosan chain is not significant, and thus, in such cases, COS can impart better performance.[21] The lower MW increases the binding strength to the membrane, and increasing the DD at lower MW further strengthens the binding. However, this increased binding can have a negative impact on the cytotoxicity, so a balance is important to ensure optimal performance.[22] Low MW of COS is also associated with increased drug capacity and drug release.[23] Water-soluble COS erodes faster, thus inducing a faster release action.[24] However, the release rate is also dependent on the size, shape, and charge of the drug.[25] Chitosan and COS both produce natural metabolites due to biodegradation without the accumulation of byproducts under the action of hepatic and bactericidal enzymes such as lysozymes.[26] So, the risk of bioaccumulation is negligible, even more so for COS, due to its shorter chains and ease of removal.[27] Like other performance factors, DD and MW influence biodegradation, as decreasing the DD at low MW increases the degradation rates.[28] Chemical modification, such as active targeting, and physical modification, such as passive targeting, are options for targeted drug delivery. However, difficulty in achieving control of passive targeting and heterogeneity of the tumors makes the external stimuli-responsive DDS a better option.[17]

The positive charge of chitosan in alkaline conditions makes it a good candidate for creating a polyelectrolyte complex (PEC) to design a drug delivery system (DDS). PECs are known to be more biocompatible and less toxic compared to chemically crosslinked hydrogels. Chemically crosslinked hydrogels may contain unreacted residues, which need to be extracted and removed to minimize cytotoxic effects.[29] Sodium carboxymethyl cellulose (CMC) is a long polysaccharide chain containing carboxylic groups that ionize to form an anion, inducing the formation of a PEC with COS. As the stability of the PEC depends on many factors, including the pH of the medium, the COS–CMC complex is a good agent for pH-sensitive release. However, the mechanical strength of the COS–CMC complex is low and thus further crosslinking with PEGDA through the UV crosslinking mechanism will enhance the stability of the DDS.[30] Also, the use of PEGDA has been seen to favor higher drug release compared to hydrogels without PEGDA.[31] Vancomycin is generally used to treat or prevent infections caused by Gram-positive bacteria in the intensive care unit (ICU) for diseases such as pneumonia, empyema, and endocarditis, among others.[32] The positive charge of vancomycin up to a pH of 8.30 makes it a useful option in terms of pH-sensitive release.[33] Furthermore, H-bonding with the PEC complexes and the temperature effect on those bonds can also be utilized to induce a temperature-sensitive response. Hence, vancomycin has been subjected to numerous pH and temperature-sensitive drug release studies.

The union of synthetic and natural polymers, introducing different functional groups, allows for tunable mechanical and biodegradable properties of the hydrogel and facilitates an external stimuli-responsive, on-demand drug delivery.[34] The development of such DDSs provides an edge over the more conventional DDSs, such as oral antibiotic tablets. Intake of such tablets can lead to a prolonged interaction with the gut flora and a subsequent decrease in the efficacy of the drug due to the development of antibiotic microbial resistance (AMR).[35] Therefore, oral administration of stimuli-responsive hydrogel can subvert the repercussions associated with such conventional DDSs, as it responds to the inflammatory site's pH, temperature, enzymes, or other factors and adjusts the intensity and frequency of its drug release without inducing off-target release.[36] Thus, in this study, we developed such an external stimuli (pH, temperature) responsive oral COS-based hydrogel and introduced another parameter – biomixing temperature, to show its effect in tuning the incorporation and release of the vancomycin hydrochloride (COVAN) drug.

In our previous study, a convenient two-stage green synthesis approach was used in depolymerizing chitosan to produce COS and to construct a COS-based PEC hydrogel (MW = 12.8 kDa, DD = 62.5%).[37] The objective of this study was to incorporate vancomycin hydrochloride into this hydrogel solution mixed at two different temperatures (4 °C and 30 °C), formed by UV-crosslinking, and to analyze the drug's pH-sensitive and temperature-sensitive release kinetics along with their antibacterial activity. To the best of our knowledge, this study is the first to utilize the biomixing temperature to tune the drug release of an external stimuli-responsive

hydrogel. The hydrogels, with and without the drug, were characterized using scanning electron microscopy (SEM), Fourier transform infrared (FTIR), thermal analysis (DSC–TGA), and X-ray diffraction (XRD) to determine the interaction of the drug with the hydrogels. These results were used to justify the drug release kinetics under different conditions.

2. Materials & methodology

2.1. Materials

Chitooligosaccharide (COS) (MW = 12.8 kDa, DD = 62.5%) was prepared as discussed in our previous work.[37] Polyethylene glycol diacrylate (PEGDA) (MW = 700 Da, Merck), Irgacure-2959 (Sigma-Aldrich), and carboxymethyl cellulose (CMC) (Thermo Fisher Scientific) were used for the hydrogel preparation. A UV radiation chamber (UVB and UVC, average intensity 10 W m^{-2}) was used for photopolymerization reactions. Glacial acetic acid (99.99%), Na_2HPO_4, KCl and KH_2PO_4 and dimethylsulfoxide (DMSO) were of reagent grade supplied by Thermo Fisher Scientific. Vancomycin hydrochloride (COVAN) drug was obtained locally from a drug store and was used to incorporate into the hydrogel. COVAN is an antibacterial prescription medicine approved by the U.S. Food and Drug Administration (FDA) for the treatment of certain bacterial infections, such as infections caused by *Clostridium difficile* and *Staphylococcus aureus*.

2.2. Hydrogel synthesis

0.5 g of COS (n = 0.0390 mmol) was dissolved in 100 mL of 1% (v/v) acetic acid solution. The pH was adjusted to 7. The solution was stirred overnight, and once the COS particles were dissolved, 1 mL of this COS solution was mixed with 5 mL of a copolymer solution containing 7.5% (w/v) of PEGDA and 4% (w/v) CMC. Polyethylene glycol diacrylate (PEGDA) is a three-dimensional chain formed due to the crosslinking of PEG monomer. Its biocompatibility, mixed with its ability to replicate the extracellular matrix, and usage in sustained/controlled drug release applications has made it an attractive choice as a physical crosslinker.[38] CMC combined with chitosan and its derivatives has shown good mechanical properties, good water retention ability, and biological activity, including wound dressing, cytocompatibility, proliferation, and differentiation of human skin cells.[39] 0.1 g of Irgacure 2959 (n = 0.4454 mmol) was dissolved in 10 mL of DMSO to prepare a 1% (w/v) solution. 137 μL of this solution was mixed with the COS solution and the copolymer solution. The mixture was mixed using a micropipette at two different temperatures (4 °C and 30 °C). Irgacure 2959 is a modified type-I photoinitiator with increased solubility. The chemical modification of type-I photoinitiators is done by introducing groups such as polyethers, hydroxyethers, and ammonium salts into the initiators. Irgacure 2959 is the most popular water-soluble initiator due to the addition of –OH groups to solubilize it.[40]

The resulting solution was cured in a UVB-UVC combination light source (100–480 nm and 10 W). The curing was done for about 2.5 hours so that it was enough to produce the hydrogel, but not too long, which would harden it. The samples mixed at 4 °C and 30 °C were labelled 4°(WD) and N(WD), respectively.

2.3. Drug incorporated hydrogel synthesis

Before UV curing, the hydrogel solution mixture comprising COS, copolymer, and the DMSO solution was mixed with 0.0667 g of COVAN (n = 0.0460 mmol) drug. Two solutions of the same composition were mixed thoroughly using a micropipette at two different temperatures (4 °C and 30 °C). The hydrogel solution mixture was then sent to a UVC–UVB light chamber (10 W m^{-2}) to be photocured into a cylindrical hydrogel (at 30 °C, 1 atm for 2 h). The samples mixed at 4 °C and 30 °C were labelled 4°(D) and N(D), respectively. The schematic of the process is shown in Fig. 1.

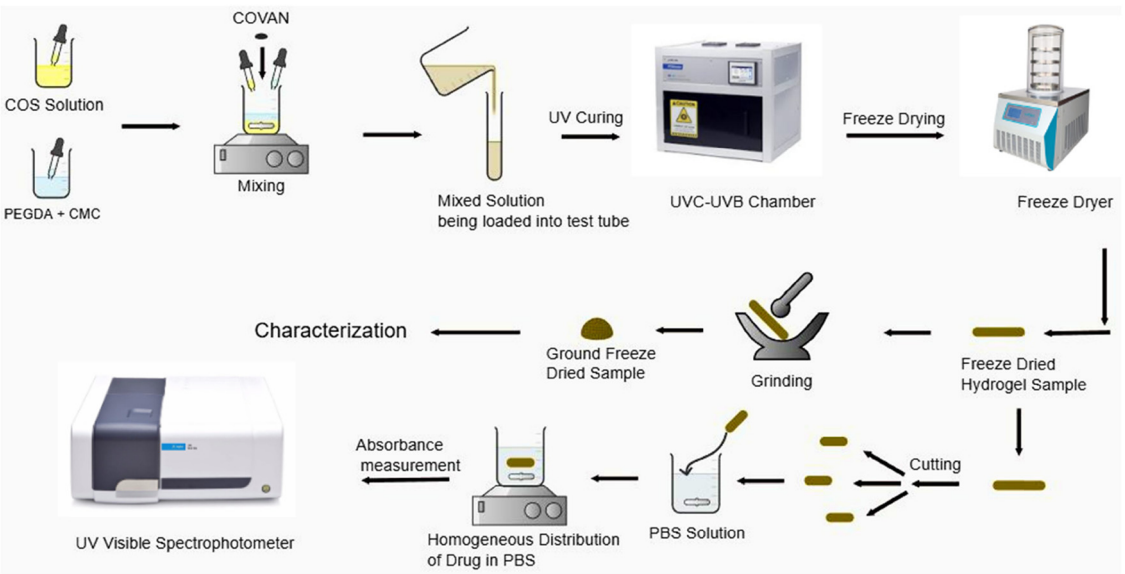

Fig. 1 The graphical methodology starting from hydrogel synthesis to characterization and application.

Even though removing organic solvents for drug delivery applications is necessary to ensure no cytotoxic effect, Ur-Rehman *et al.* showed that DMSO used at low concentrations (<5%) ensures safe cytotoxic levels.[41] Therefore, DMSO was a valuable agent in producing a soluble mixture of Irgacure-2959 while maintaining no cytotoxic effect as its concentration was maintained at 2.23% (v/v).

2.4. Characterization of the drug-free hydrogel sample

Both of the drug-free samples were freeze-dried (−55 °C, 0 torr for 24 h). The freeze-dried samples were crushed into small powders and analyzed using a diamond tip ATR-FTIR over wavenumbers ranging from 4000 to 400 cm^{-1} at a resolution of 4 cm^{-1} and a total of 64 scans.

2.5. Characterization of the drug incorporated hydrogel sample

The drug-loaded hydrogel samples were freeze-dried and crushed exactly like the drug-free samples, and also analyzed using a diamond tip ATR-FTIR over wavenumbers ranging from 4000 to 400 cm^{-1} at a resolution of 4 cm^{-1} and a total of 64 scans. This gave the functional group analysis of the hydrogel to confirm the incorporation of vancomycin.

XRD analysis was conducted on the Rigaku SmartLab SE, which consisted of a Cu-Kα source (with a nickel filter) and was operated at 40 kV and 30 mA. The wavelength was 1.5 Å, the sweep rate was 1.2° min^{-1}, and the scattering angle (2θ) range was 5–80°.

DSC and TGA analyses of 4°(WD), *N*(WD), *N*(D), 4°(D), and vancomycin were carried out using a Netzsch STA 449F3 instrument under a nitrogen atmosphere (purge flow rate of 20 mL min^{-1}). The heating rate was 30 °C min^{-1} over the range 0–700 °C. The DSC–TGA experiments were carried out using 10 mg of each of the samples placed in Al_2O_3 pans.

N(WD), 4°(WD), *N*(D) and 4°(D) were freeze dried for 24 h (−55 °C and 0 torr). The freeze-dried samples were cut and mounted on separate SEM stubs and coated with a 10 nm layer of gold using a mini sputter coater by Quorum Testing. The images were taken at a voltage of 10.0 kV in the EVO 18 SEM machine at three different magnifications (500×, 1k× and 5k×). Using SEM images, the surface morphology and texture were visualized.

2.6. Equilibrium swelling ratio

Freeze-dried *N*(WD), 4°(WD), *N*(D), and 4°(D) samples were weighed and put into PBS of pH 1.2 and 6.8 separately at two different temperatures (30 °C and 37 °C). After 24 h, the samples were taken out, and the excess solution was blotted out using filter paper. The samples were then weighed to determine the equilibrium swelling ratio (ESR). If the initial and final weight of the sample were W_0 and W_f, respectively, then,

$$\text{Equilibrium swelling ratio}\ (\%) = \frac{W_f - W_0}{W_0} \times 100\%$$

For swelling kinetics, the samples were weighed at different time intervals (t = 5, 10, 20, 30, 40, 50, 60, 120 minutes) to determine the swelling ratio at these time intervals.

2.7. Drug release kinetics

Each of the freeze-dried cylindrical *N*(D) and 4°(D) samples was cut into three pieces (1 cm × 1 cm) and submerged in PBS buffer under the required conditions (pH = 1.2, 6.8, and T = 30 °C, 37 °C). The absorbance was measured at a wavelength of λ = 280 nm against a base of PBS at pH = 1.2 and 6.8. The submerged sample, along with the beaker, was kept under constant shaking to ensure homogeneous distribution of the drug. The absorbance readings at different time intervals, t = 15, 30, 45, 60, 120, 240, 1440 min, were converted to the total amount of drug release using the calibration data for the corresponding pH (1.2 and 6.8).

The drug release data were fit into 5 different models to check which model described the kinetics best. The models are zero and first order models, the Higuchi model, the Hixson–Crowell model, and the Korsmeyer–Peppas model. Details of the models are discussed in the ESI.†

2.8. Determination of antibacterial activity by disc diffusion and well diffusion

The suppression of bacterial proliferation by COS–CMC–PEGDA hydrogel was evaluated using disc-diffusion and well-diffusion assays, as outlined by the Kirby–Bauer disc diffusion susceptibility test protocol, with specific modifications. The antimicrobial efficacy of COS–CMC–PEGDA hydrogel was evaluated against a Gram-negative bacterium (*K. pneumonia* ATCC 13883) and a Gram-positive bacterium (*B. cereus* ATCC 14579). Approximately 20 mL of Mueller–Hinton agar was dispensed into sterile Petri dishes to create the base plates. About 0.1 mL of standard bacterial stock suspensions (10^8–10^9 cfu mL^{-1}) was inoculated onto the base plates using a sterile cotton swab. Two stock solutions of 10 mg mL^{-1} of COS–CMC–PEGDA hydrogel, fabricated at two different temperatures and loaded with vancomycin hydrochloride, were prepared using PBS. Additionally, 6 mm-diameter sterilized filter paper discs were submerged in the COS–CMC–PEGDA hydrogel solutions and subsequently positioned on the surface of the bacterial test plates. In the case of the well diffusion test, wells were prepared aseptically on the inoculated plates and 200 microliters of each sample were placed in the wells. PBS was used as a negative control, and vancomycin hydrochloride was used as a positive control in each case. Following a 24-hour incubation period, the diameters of the inhibition zones were measured. The disc diffusion test and the well diffusion test revealed antibacterial activity solely against *K. pneumonia* and *B. cereus* using the same concentration of COS–CMC–PEGDA hydrogel. The concentration was 10 mg mL^{-1}. After 24 hours of incubation, growth was observed on each plate.

2.9. Determination of MIC and MBC using the resazurin test

2.9.1. Bacterial strains. The current investigation evaluated Gram-negative bacteria *K. pneumonia* ATCC 13883 against COS–CMC–PEGDA hydrogel fabricated at two different temperatures and loaded with vancomycin hydrochloride. The MIC was subsequently established by observing the color change.

2.9.2. Preparation of the resazurin reagent. Resazurin was made at a concentration of 0.015% by dissolving 0.015 g,

spinning, and filtering (0.22 μm), and then storing it at 4 °C for no more than 2 weeks.

2.9.3. Preparation of standardized inoculum. The inocula were prepared according to the CSLI guidelines, with the OD600 value calibrated to 10^8 CFU mL^{-1} for each bacterium based on a calibration curve. 96-well plates were prepared for the evaluation of COS–CMC–PEGDA hydrogel. The COS–CMC–PEGDA hydrogel was transferred and mixed from columns 1–10 of rows 1, 3 and 5 utilizing a multichannel pipette, resulting in 100 μL per well. Double serial dilutions from columns 1 to 10 produced test values ranging from 10 to 0.0195 mg mL^{-1} for the different COS–CMC–PEGDA hydrogels fabricated at two different temperatures and loaded with vancomycin hydrochloride. The standard bacterial suspension was subsequently diluted one hundred times in MHB broth. Fifty microliters of titrated bacterial suspension (approximately 5×10^5 CFU mL^{-1}) was administered to all COS–CMC–PEGDA hydrogels and control wells. The complete preparation and administration of the OD-adjusted bacteria required under 15 minutes. Resazurin (0.015%) was introduced to all wells (30 μL per well) following 24 hours of incubation at 37 °C, and the plate was allowed to rest for an additional 4 hours before assessment for colorimetric alteration. Upon the conclusion of the incubation period, the MIC value was utilized for the columns exhibiting no alteration in the blue resazurin coloration (Fig. S2, ESI†). The MBC can be determined by plating wells at concentrations exceeding the MIC. The MBC was determined by plating the well contents that exhibited no colony development. Serial dilutions were conducted on the wells displaying growth inhibition to ascertain the final concentration at which the bacteria perished.

2.10. Statistical analysis

Each experiment was performed at least in triplicate. All data were shown as means ± standard deviation. IBM SPSS Statistics software version 25 was used to analyze results with a *p*-value of 0.05 using one-way ANOVA.

3. Results and discussion

3.1. Hydrogel characterization

Fig. 2 shows the interaction between the components of the hydrogel and the hydrogel itself formed at two different temperatures (30 °C and 4 °C). The absorption band at 2867 cm^{-1} is

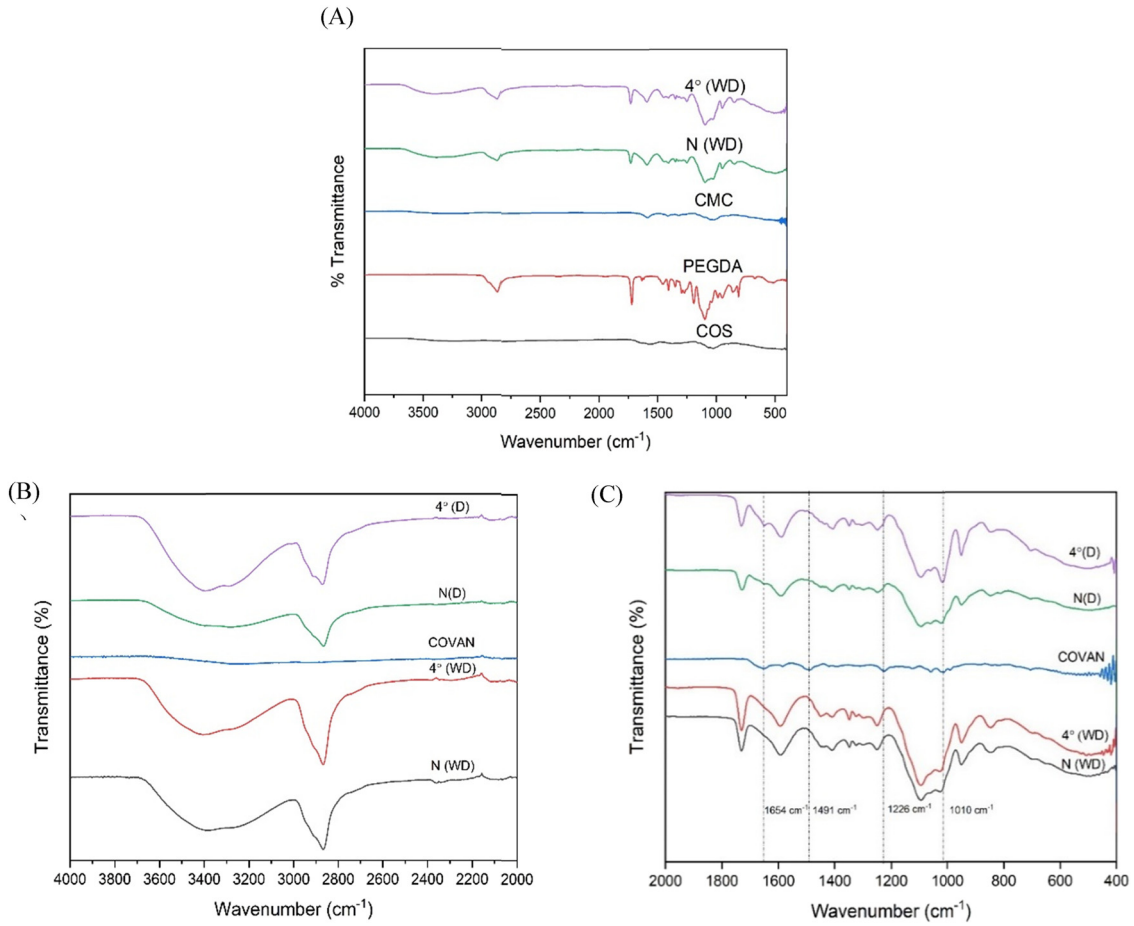

Fig. 2 (A) Comparison of the FTIR spectra of the different components of the hydrogels and the hydrogel itself. Comparison of the FTIR spectra of the different components of the drug-loaded hydrogels and the hydrogel in (B) the wavenumber range of 2000–4000 cm^{-1} and (C) the wavenumber range of 400–2000 cm^{-1}.

due to symmetric stretching of the –CH in the hydrogel. A similar absorption band can be seen for PEGDA.

The peak at 1730 cm^{-1} is assigned to the stretching of –C═O in unsaturated esters. The small absorption band at 3380 cm^{-1} comes from the stretching of the –OH bonds, which can be seen for COS and CMC as well. The peak at 1594 cm^{-1} originates from the stretching of the –N–H bond in the $RCONH_2$ group. This peak is evident for COS as well. The peaks at 1453 cm^{-1} for hydrogels and PEGDA are due to the methyl–CH asymmetric stretching. The 1407 cm^{-1} peak corresponds to stretching of –CH in the $–CH–CH_2$ group. The peaks at 1350 cm^{-1} and 1243 cm^{-1} are assigned to the stretching of methyne –CH bend and –CN stretching, respectively. Similar peaks can be found for PEGDA (1350 cm^{-1}) and COS (1243 cm^{-1}). The peak at 1096 cm^{-1} is associated with –O– bond stretching in esters for PEGDA and the hydrogels. The peaks at 950 cm^{-1} and 847 cm^{-1} are attributed to C═C stretching and the presence of the glucopyranose ring. This is confirmed by Tabassum *et al.*,[37] where the characteristic absorption peaks for the COS–PEGDA–CMC-based hydrogel were found at 3383, 2867, 1730, 1590, 1409, 1250, 1096, 950, and 847 cm^{-1}.[37] The effect of temperature on the hydrogel structure, however, was not investigated. Fig. 2 shows that there isn't much difference in the absorption peaks of *N*(WD) and 4°(WD) hydrogels. Khaleghi *et al.* also showed that the effect of temperature is evident in the changes of the swelling property, surface roughness, and network topology, but not in the structure of two hydrogels formed at two different temperatures.[42]

The absorption spectra for *N*(D) and 4°(D) are quite similar to the absorption spectra for *N*(WD) and 4°(WD) (Fig. 2B and C). However, the presence of some small yet additional peaks can be seen for *N*(D) and 4°(D) due to the interaction between the drug vancomycin (Covan) and the hydrogels. Such interactions are represented by new peaks at 1654, 1491, 1226, and 1010 cm^{-1}. The peak at 1654 cm^{-1} is characteristic of the $R–CONH_2$ group. The peak at 1491 cm^{-1} is due to the –C═C–C aromatic ring stretch. The stretching of –C–H bonds in the aromatic ring corresponds to the peak at 1226 cm^{-1}. The peak at 1010 cm^{-1} is assigned to the the –CN stretching. The presence of the characteristic peaks of vancomycin in *N*(D) and 4°(D) confirms the incorporation of the drug in the hydrogels.

3.2. SEM morphology

SEM images depict a comparison of the hydrogels with and without the incorporation of the drug. In Fig. 3(A), the *N*(WD) hydrogels exhibit a fibrous nature due to the formation of a porous structure which resembles the extracellular matrix (ECM).

In Fig. 3(C), the 4°(WD) also exhibits a fibrous nature. However, the fibrous nature of 4°(WD) is dominant compared

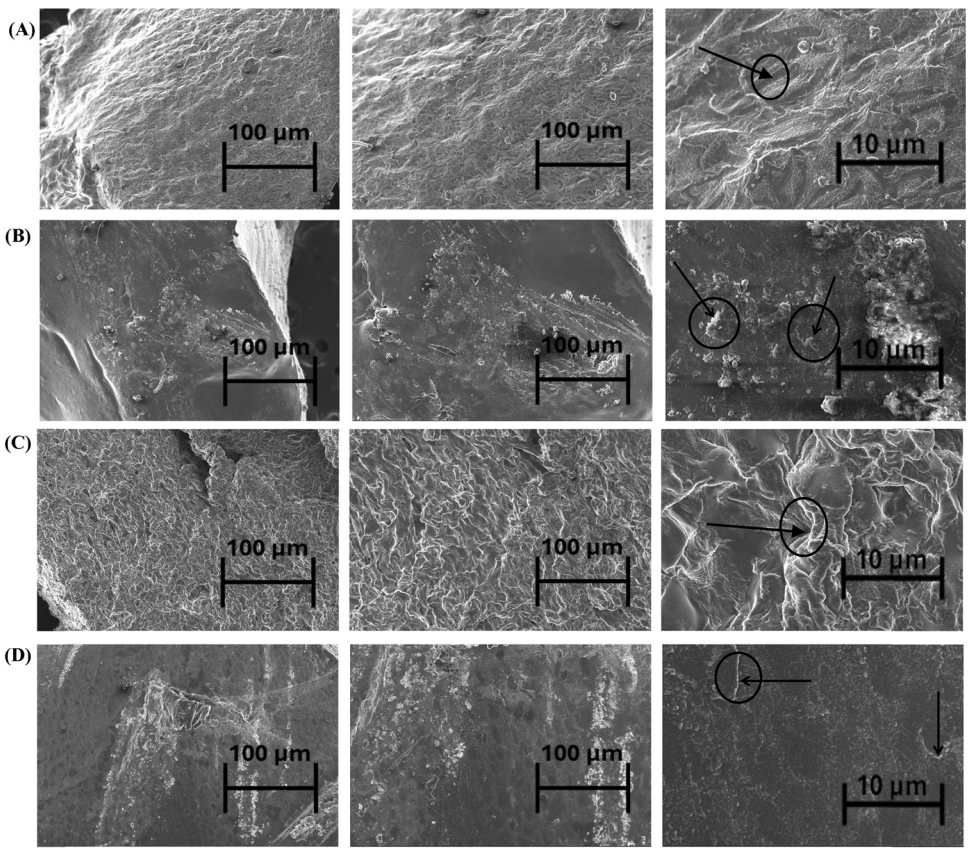

Fig. 3 Scanning electron microscope images of the surface morphology at 500×, 1k× and 5k× of (A) *N*(WD); (B) *N*(D); (C) 4°(WD) and (D) 4°(D). The black arrows and circles in 4°(WD) and *N*(WD) indicate the voids in the hydrogel surface. In contrast, the black arrows and circles in 4°(D) and *N*(D) indicate the loaded drug.

to *N*(WD). This could be explained by the fact that photoinitiator concentration and temperature influence the crosslinking density of PEGDA. Scaffold/hydrogel formed at a lower temperature showed higher failure stress compared to the higher temperature hydrogel, indicative of the greater crosslinking density at lower temperature.[43] The SEM images (Fig. 3(A) and (D)) at 5k× magnification of *N*(D) and 4°(D) depict the incorporation of the drug into the pores of the hydrogel, indicated by the black arrows and circles. The incorporation of the drug into the 4°(D) is higher compared to *N*(D), where the surface of the 4°(D) is much smoother compared to *N*(D). This indicates that the 4°(D) lost its fibrous and porous structure more compared to *N*(D). Setiyorini *et al.*[44] also investigated the effect of temperature on the drug loading capacity of the NIPAAm copolymer. The findings show that the drug loading capacity for a 2 wt% drug solution was 17.5% and 10.4% at 10 °C and 22 °C, respectively.[44] The greater incorporation of the drug indicates that the 4°(WD) had a higher pore volume than *N*(WD). Higher pore volume allowed for greater uptake of the drug through diffusion.

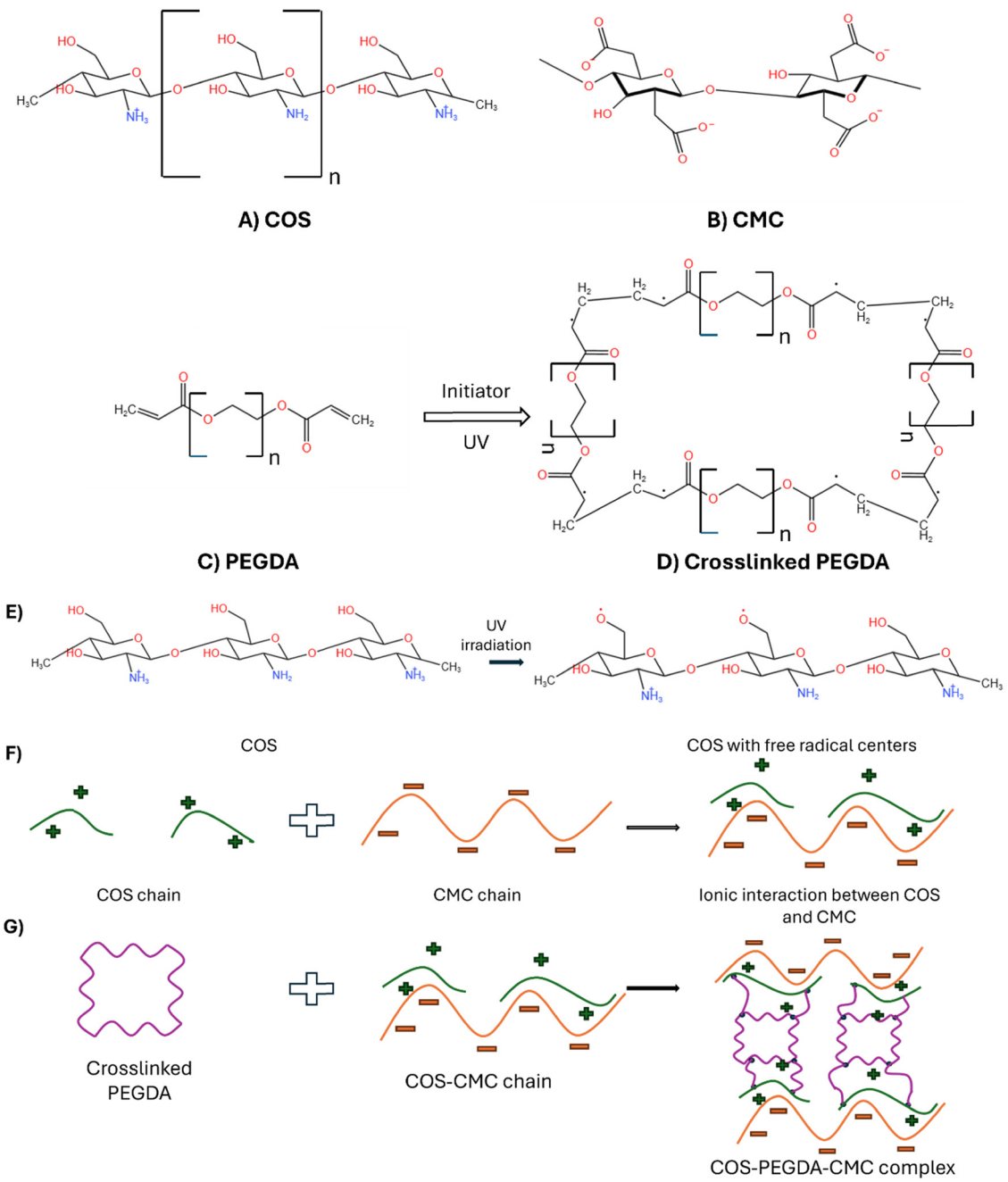

Fig. 4 Chemical structure of (A) COS; (B) CMC; (C) PEGDA; (D) crosslinked PEGDA due to UV photocrosslinking; (E) free radical formation on the COS chain due to UV irradiation; (F) ionic interaction between COS and the CMC chain; and (G) interaction between crosslinked PEGDA and the COS–CMC complex to form a COS–PEGDA–CMC complex.

3.3. Interactions between covan and COS hydrogel

3.3.1. Mechanism of interaction. Tabassum *et al.*[37] have previously proposed the reaction mechanism between chitooligosaccharide (COS)–polyethylene glycol diacrylate (PEGDA)–carboxymethyl chitosan (CMC) complex.[37] Based on this reaction mechanism, the interaction of vancomycin with the COS–PEGDA–CMC complex can be postulated (Fig. 4).

Due to the presence of protonated amine groups in COS and negative charge on CMC, the COS–CMC complex formation is because of ionic interaction between these two charged groups. As reported by Zhu *et al.*[45] this is similar to the CMC–QCS complex formation, where COS is a derivative of QCS with shorter chains.[45] Under UV irradiation, PEGDA chains crosslink owing to a free radical mechanism. These crosslinked PEGDA chains bond to the already formed COS–CMC complex with free radical centers under UV irradiation. This reaction mechanism forms a crosslinked COS–PEGDA–CMC complex with some free negative charge centers on the CMC chains. Vancomycin, which has an isoelectric point of pH = 8.30 with a net positive charge at a pH of <8.30, forms a dipole–dipole interaction with these free negative charge centers[33] shown in Fig. 5. Gustafson *et al.*[7] showed that vancomycin forms ionic interactions with negatively charged groups in hydrogel formation, which influences the swelling ratio, and drug release kinetics.[7] This reaction mechanism has been graphically represented in Fig. 5.

3.3.2. X-ray diffraction peaks. The crystallinity of the hydrogels was analyzed by X-ray diffraction analysis (Fig. 6). The unloaded hydrogel *N*(WD) showed a peak at 21°, indicating a moderate amorphous nature. It did not retain the very amorphous nature of COS and CMC. This is mainly because the hydrogen bonds, both intra and intermolecular, to the CMC and COS are destroyed due to the ionic interaction between them, which in turn reduces their crystallinity.[46]

The peak of *N*(WD) is characteristic of the diffractogram of the PEGDA crosslinker, another component of the hydrogel.[47] However, the diffractogram of 4°(WD) retains the amorphous nature of COS and CMC but does not retain the crystallinity of PEGDA. This is because the degree of crystallinity increases with increasing polymerization temperature.[48,49] Also, for chitosan and its derivatives, the hydrogen bonds are stronger at lower temperatures, thereby retaining their crystallinity and influencing the crystallinity of the hydrogel.[50] The vancomycin drug has a characteristic peak at $2\theta = 13.2°$. The characteristic peak of 4°(D) is at $2\theta = 15.38°$, which falls between the peaks for 4°(WD) and vancomycin, indicating successful incorporation of the drug. The crystalline nature of the *N*(D) disappears after incorporation of the drug. The absence of a peak at $2\theta = 13.2°$

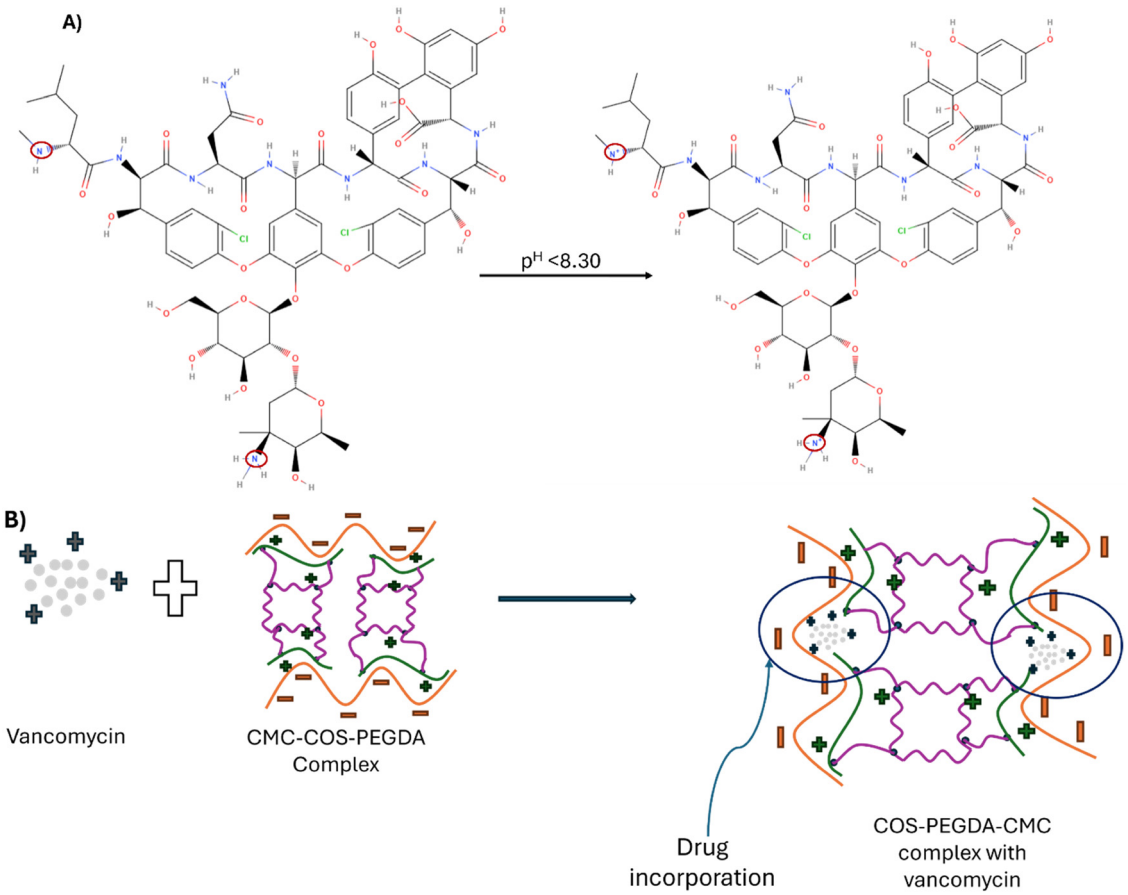

Fig. 5 (A) Charging of the vancomycin structure at a pH below 8.30; (B) ionic interaction between charged vancomycin and the COS–CMC–PEGDA complex for the incorporation of drug into the hydrogel.

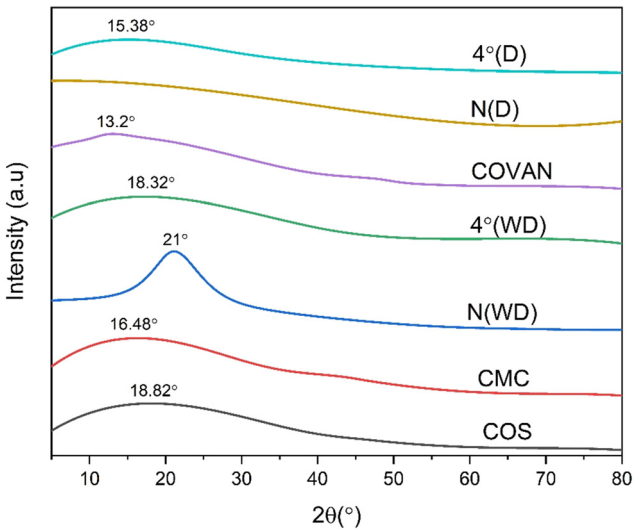

Fig. 6 Comparison of the X-ray diffractogram of the different components of the hydrogel, unloaded hydrogels, and drug-loaded hydrogels.

for both *N*(D) and 4°(D) confirms the lack of free drug in the sample and thereby indicates the successful incorporation of the drug. The crystallinity index (CI) of 4°(D) is 12.24%, which is lower than the CI of *N*(D) at 17.74%. The crystalline/amorphous ratio for 4°(D) and *N*(D) is 0.139 and 0.216, respectively, further indicative of the greater amorphous nature and the greater incorporation of the vancomycin drug in 4°(D) hydrogel over *N*(D) hydrogel.

3.3.3. DSC–TGA analyses. The DSC results further confirm the interaction between vancomycin and the hydrogels. The 4°(WD) and *N*(WD) have endothermic peaks at 390 °C and 385 °C, respectively, corresponding to their melting temperatures T_m (Fig. 7(B)). The increased melting temperature of 4°(WD) can be attributed to a greater crosslinking density and strengthening of the H-bonds at lower temperatures.[50]

The endothermic peak for the unloaded polymer in the range of 380–390 °C is due to the presence of COS, as it exhibits an endothermic peak at this range.[37] No endothermic peaks associated with the evaporation of water molecules were noticed, as the samples tested were freeze-dried previously. The incorporation of the drug shifted the exothermic and endothermic peaks both to the right because of the ionic interaction and hydrogen bonding between vancomycin and the unloaded polymer, which improved its thermal stability. The interaction between the drug and the polymer is further confirmed by the flattening of the curve, as the vancomycin curve does not exhibit any significant peak.

For thermogravimetric analysis, two distinct peaks can be observed for both the loaded and the unloaded polymers (Fig. 7(D)). One in the range of 280–290 °C corresponding to about 30% mass loss, which can be attributed to the loss of the cyclic moiety from the poly-electrolyte complex.[51] Another peak in the range of 380–400 °C, responsible for 40–45% mass loss, is due to the degradation of the crosslinked hydrogel structure. The loss of amide or ether linkages may be responsible for the degradation at this range.[52] The DTG curve further confirms the better crosslinking of 4°(WD) compared to *N*(WD), as the mass loss occurs at a higher temperature for 4°(WD). The incorporation of vancomycin also causes mass loss at a higher temperature for both *N*(D) and 4°(D) compared to *N*(WD) and 4°(WD), respectively.

3.4. Equilibrium swelling ratio and swelling kinetics

The equilibrium swelling ratio (ESR) at different pH and temperature is influenced by the ionic interaction between the $-NH_2$ amine group in chitooligosaccharide (COS) and the –COOH group in carboxymethyl chitosan (CMC). The pK_a values of chitosan and CMC are 6.3 and 4.2, respectively.[53] However, the pK_a of chitosan varies with its change in degree of deacetylation (DD) and molecular weight (MW).[54] For a DD of 62.3% and an MW of 12.3 kDa, chitosan represents COS. At this DD and MW, the pK_a value is in the range of 6.2–6.5.[37]

For the hydrogels 4°(WD) and *N*(WD), the ESR has a higher value at pH 6.8 compared to at pH 1.2 at both temperatures (30 °C and 37 °C) as seen in Fig. 8(A). At pH 1.2, there is almost an equal number of carboxylate acid –COOH groups and carboxylated anions $-COO^-$ groups. The amine groups are also protonated, forming $-NH_3^+$ ends. These attract the carboxylate anions ($-COO^-$), which compress the hydrogel structure and thereby cause deswelling.[55] On the other hand, at pH = 6.8, the deionization of the ammonium group leads to the formation of $-NH_2$ groups with carboxylate anions present in the structure. Due to the absence of protonated groups, these anions ionically repel each other, leading to a higher ESR for this pH.[5]

To analyze the effect of temperature on the swelling/deswelling of the hydrogels, the lower critical solution temperature (LCST) can provide a reasonable explanation. A temperature above the LCST can result in the blockage of the diffusion channel and thus cause deswelling.[56] The LCST of the chitosan and CMC mixture is in the range of 55–65 °C at various pH values.[57] The effect of the PEGDA's concentration on the variation of the LCST of PNIPAAM hydrogel has been reported by Son and Lee.[58] For almost all molecular weights, the increase in PEGDA concentration caused an increase in the LCST of the hydrogel, except for liquid PEGDA, which caused a decrease in the LCST.[58] As the PEGDA used for hydrogel formation was liquid, it may have caused the LCST to decrease to a range of 30–37 °C. For 4°(WD) hydrogel, at a pH value of 1.2, the increase in temperature from 30 °C to 37 °C resulted in a decrease in ESR. This is probably because the LCST was in the range of 30–37 °C, and crossing the LCST resulted in deswelling. However, at a pH of 6.8, an opposite trend was observed where increasing the temperature from 30 to 37 °C increased the ESR. Pei *et al.*[59] reported that for pH $\ll$ 7, increasing the pH resulted in a decrease of the LCST of PNIPAAM and P(NIPAAm-*co*-AAc) hydrogels, but for pH $>$ 7, the increase in pH increased the LCST.[59] As this PNIPAAM and P (NIPAAm-*co*-AAc) hydrogel has free $-RCONH_2$ amide groups and $-COO^-$ carboxylate anions, the COS–PEGDA–CMC complex can be predicted to behave similarly. Therefore, at a higher pH, the LCST could have been above the range of 30–37 °C for each hydrogel. As at lower temperatures the intra and intermolecular hydrogen bonds are stronger, the hydrogel structure is more compact which resulted in deswelling at 30 °C. For *N*(WD) hydrogel, increasing

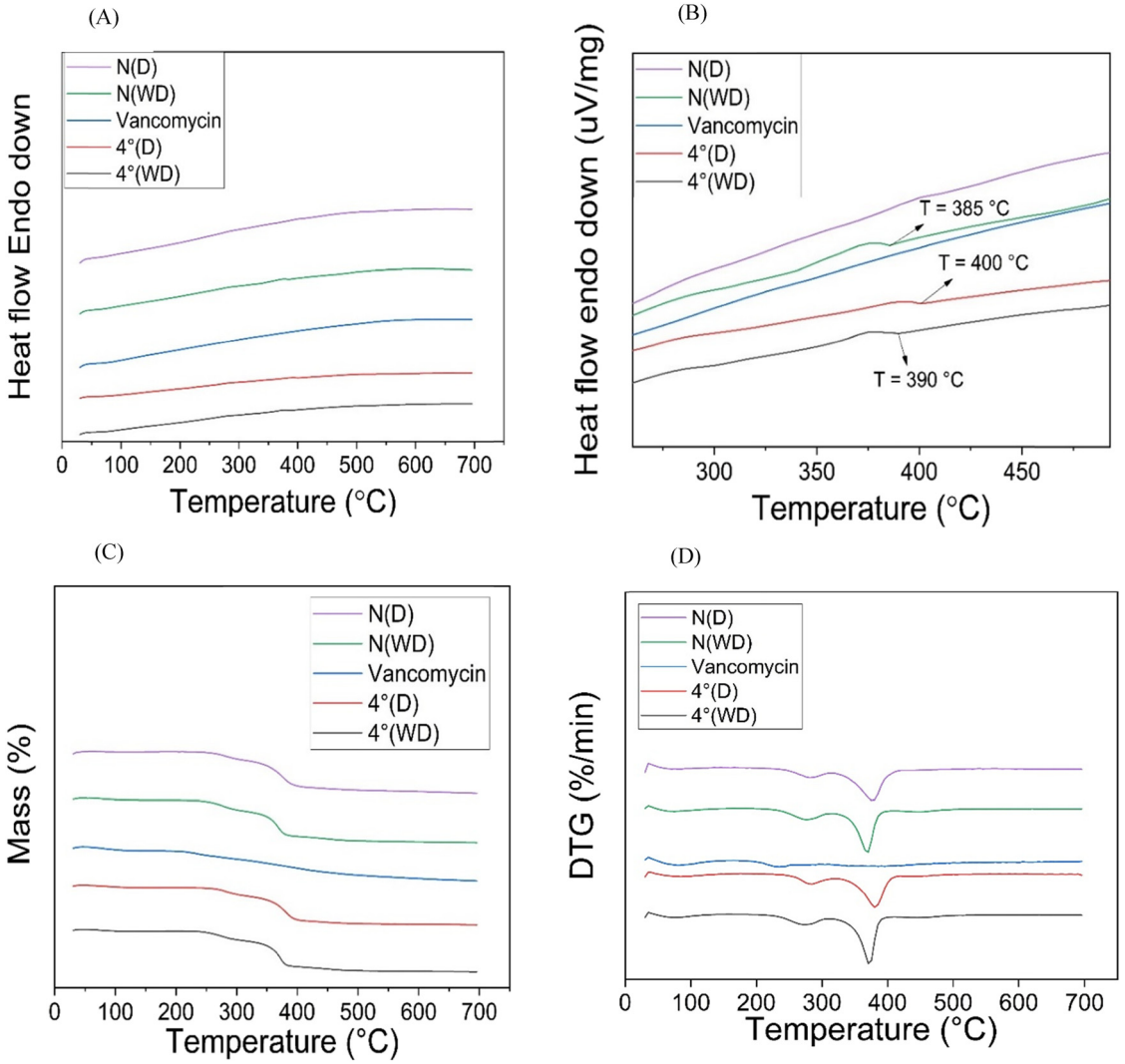

Fig. 7 (A) DSC of loaded and unloaded polymers and the vancomycin drug, (B) enlarged section of the DSC curve, (C) TGA curve of the loaded and unloaded polymers and (D) differential thermal gravimetric analysis showing major peaks for mass loss.

the temperature from 30 °C to 37 °C at a pH of 1.2 resulted in an increase of the ESR contrary to the 4°(WD) hydrogel. This could be explained by the fact that as *N*(WD) has a lower crosslinking density compared to 4°(WD), crossing the LCST disintegrates the structure. Thus, the blocking of the diffusion pore channels was not significant anymore in the drug release amount.

The swelling kinetics at pH 1.2 at 30 °C provides a comparison between the swelling of each hydrogel under a particular condition. The swelling ratio for hydrogels increases in the order 4°(WD) < *N*(WD) (Fig. 8(B)). The higher amount of drug incorporation leads to the lowest swelling for 4°(D) as indicated by SEM morphology. The drug-incorporated hydrogels have lower swelling compared to drug-free hydrogels due to decreased porosity. The *N*(WD) has higher swelling compared to 4°(WD) due to the greater crosslinking density of 4°(WD).

3.5. Controlled release kinetics

The drug release kinetics for both the hydrogels, *N*(D) and 4°(D) have been simulated in PBS of pH 1.2 and 6.8 representative of the gastric (SGF) and intestinal (SIF) fluid, respectively (Fig. 9). For *N*(D) hydrogel, the cumulative drug release (%) was higher at pH 1.2 compared to pH 6.8. At 30 °C, the percentage drug release was 41% at pH 1.2 and 24% at pH 6.8, respectively after 24 h.

The stability of vancomycin is influenced by the pH range. At a pH of 4.6–7.8, vancomycin is more stable due to its interaction with carboxylate –COO– anions.[60] At lower pH, the positive $-NH_3^+$ groups attract the COO^- anions. As fewer carboxylate anions are formed at lower pH compared to ammonium cations, the free ammonium cations repel the positively charged vancomycin drug, resulting in a greater release under this condition.[61] However, at higher pH, the ammonium cations revert to uncharged amine $-NH_2$ groups, leaving a surplus of $-COO^-$ anions. These attract the positively charged vancomycin, leading to greater stability and slower release. For both simulated gastric fluid (SGF) and simulated intestinal fluid (SIF), the fraction of drug release decreases with the increase in temperature for *N*(D). At pH 1.2, the percentage of

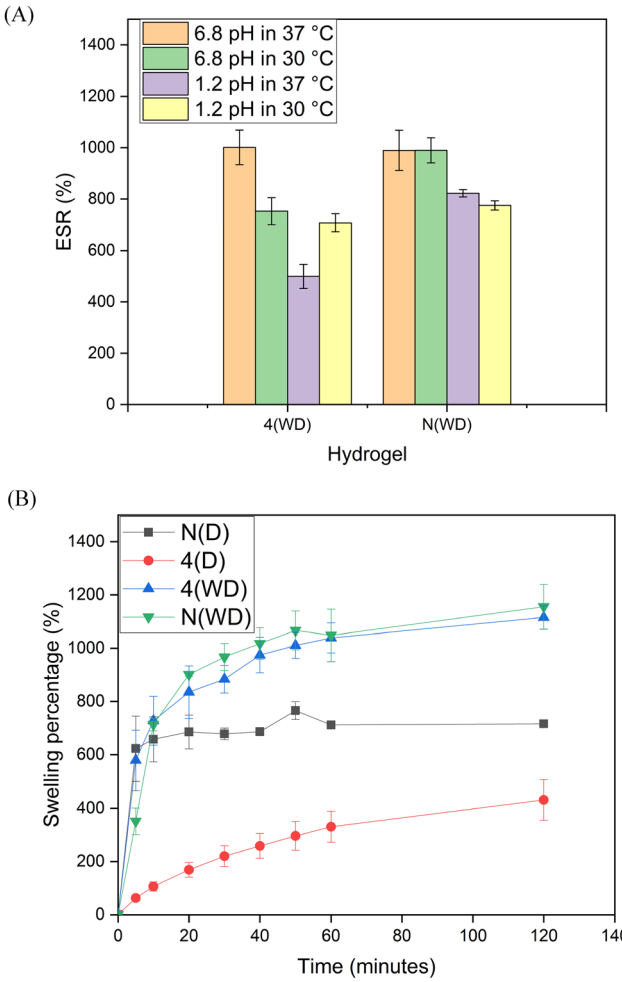

Fig. 8 (A) Equilibrium swelling ratio (ESR) of the hydrogels at different conditions. (B) Swelling kinetics of each hydrogel at pH 6.8 at 30 °C. The error bars indicate standard error.

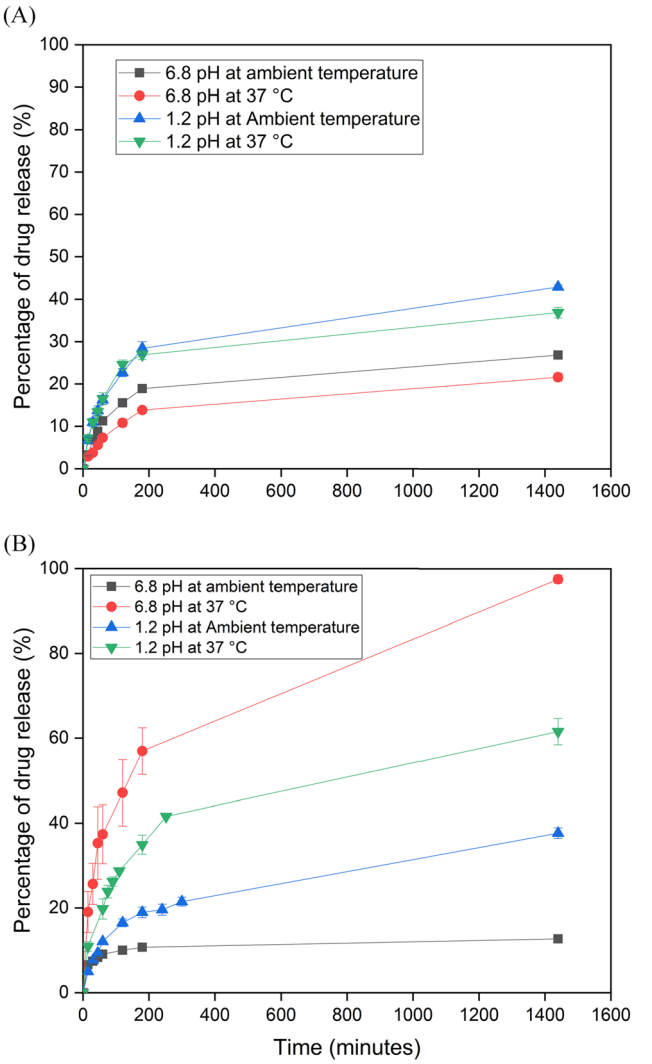

Fig. 9 pH sensitive and temperature sensitive controlled drug release kinetics of (A) *N*(D) hydrogel and (B) 4°(D) in simulated gastric (pH 1.2) and intestinal fluid (pH 6.8). The error bars indicate standard error.

drug released is 35% at 37 °C compared to 41% at 30 °C after 24 h. However, the opposite has been observed for 4°(D). Low temperature of formation might have resulted in the preservation of additional intra- and intermolecular hydrogen bonds between vancomycin and the hydrogel porous matrix for 4°(D). Therefore, at higher temperatures, a combination of faster diffusion mechanisms and the breakage of hydrogen bonds might have resulted in higher release. In the drug release data for 4°(D) at pH 6.8 and 37 °C, an anomaly is observed, with the drug release reaching about 97% after 24 hours due to the drug release mechanism following first-order kinetics (Table 1). Except for the conditions of 37 °C and 1.2 pH, the drug release amount for 4°(D) was significantly different compared to *N*(D) for all other conditions (p value <0.05) (Table S1, ESI†).

The drug release data for all other conditions followed the Korsmeyer–Peppas model. The n values of the Korsmeyer–Peppas model classify the drug release into 3 types.[62] For $n \leq 0.5$, the drug release follows a simple Fickian diffusion mechanism (case I). For $n \geq 1$, the drug release follows a case-II transport, where the polymer relaxation influences guest molecules' movement in the matrix. For $0.5 < n < 1$, the drug release is influenced by both simple Fickian diffusion and polymer relaxation. As for most conditions, the n value is less than 0.5 (case I) (Table 1); therefore, only the Fickian diffusion mechanism influenced the transport. In this case, the solvent penetration rate is much greater than the polymeric chain relaxation.[63] This might have been due to the transition temperature (T_g) of the hydrogels being lower than 30 °C and 37 °C, causing a rubbery state and inducing easy solvent penetration. Therefore, the swelling behavior and drug release behavior of the hydrogels did not correspond.

3.6. Antibacterial activity

This study evaluated a 10 mg mL^{-1} of chitooligosaccharide (COS)–carboxymethyl chitosan (CMC)–polyethylene glycol diacrylate (PEGDA) hydrogel against a Gram-negative bacterium (*K. pneumoniae* ATCC 13883) and a Gram-positive bacterium (*B. cereus* ATCC 14579). The COS–CMC–PEGDA hydrogel, fabricated at two different temperatures and loaded with

Table 1 Correlation coefficient, rate constants, Korsmeyer–Peppas model constants for the drug release data of *N*(D) and 4°(D) hydrogels under different conditions

	Conditions		Zero order		First order		Higuchi model		Hixson–Crowell model		Korsmeyer–Peppas model	
Hydrogel	pH	Temperature (°C)	Correlation coefficient (r^2 value)	Rate constant k_o (min^{-1})	Correlation coefficient (r^2 value)	Rate constant k_1 (min^{-1})	Correlation coefficient (r^2 value)	Higuchi dissolution constant k_H (min$^{-1/2}$)	Correlation coefficient (r^2 value)	Rate constant k_o (min^{-1})	Correlation coefficient (r^2 value)	*n* value
N(D)	6.8	30	0.628	3×10^{-6}	0.6712	2×10^{-4}	0.8356	2×10^{-4}	0.6569	1×10^{-5}	**0.8536**	0.434
		37	0.7128	3×10^{-6}	0.786	1×10^{-4}	0.8937	1×10^{-4}	0.734	1×10^{-5}	**0.90**	0.46
	1.2	30	0.6824	5×10^{-6}	0.759	3×10^{-4}	0.8784	2×10^{-4}	0.7342	3×10^{-5}	**0.9147**	0.4012
		37	0.5361	4×10^{-6}	0.60	2×10^{-4}	0.7664	2×10^{-4}	0.5781	2×10^{-5}	**0.8535**	0.3232
4°(D)	6.8	30	0.339	9×10^{-7}	0.6428	4×10^{-5}	0.5674	5×10^{-4}	0.3507	4×10^{-6}	**0.9291**	0.156
		37	0.6358	1×10^{-5}	**0.979**	2×10^{-3}	0.8441	5×10^{-4}	0.9107	1×10^{-4}	0.9737	0.3776
	1.2	30	0.8526	2×10^{-5}	0.9102	7×10^{-4}	0.934	3×10^{-4}	0.866	8×10^{-5}	**0.9697**	0.5038
		37	0.647	8×10^{-6}	0.817	7×10^{-4}	0.8847	4×10^{-4}	0.7752	5×10^{-5}	**0.9718**	0.33

vancomycin hydrochloride, exhibited very high antibacterial activity in the well diffusion test and disc diffusion test against *B. cereus*, as evident from the inhibition zone measuring between 19 and 29 mm, as illustrated in Fig. S1 (ESI†). But against *K. pneumoniae*, the antibacterial activity decreased dramatically. Several studies have been reported on the contrasting efficacy of vancomycin for Gram-positive and Gram-negative bacteria. Vancomycin exhibits significant efficacy against Gram-positive bacteria by obstructing cell wall synthesis through its binding to the peptidoglycan precursor, particularly the D-alanyl-D-alanine terminus, an essential element of the Gram-positive bacterial cell wall. In contrast, the outer membrane of Gram-negative bacteria hinders vancomycin from accessing its target.[64] Gram-positive bacteria possess a robust cell wall predominantly made of peptidoglycan, accessible to the external environment. Vancomycin readily penetrates and attaches to the D-alanyl-D-alanine terminal in these bacteria, obstructing cell wall formation and resulting in cell death.[65] But in the case of Gram-negative bacteria, they possess a slender peptidoglycan layer situated between an inner membrane and an outer membrane. The outer membrane, consisting of lipopolysaccharides, is a barrier that inhibits big compounds such as vancomycin from traversing it and accessing the peptidoglycan layer.[66] This could be the reason why the zones of inhibition obtained in these tests for *N*(D), 4°(D), and the positive control against Gram-positive bacteria are much greater than against Gram-negative bacteria. 4°(D) performed better than *N*(D) in every aspect due to its higher drug release (%) and better incorporation of the drug compared to *N*(D). Compared with the positive control (vancomycin hydrochloride), it was observed that 4°(D) showed nearly similar activity (Table 2). The antibacterial activity for 4°(D) was significantly higher compared to *N*(D) for *B. cereus* for both disc diffusion and well diffusion tests ($p < 0.05$).

3.6.1. MIC and MBC determination. Resazurin served as an oxidation–reduction indicator for assessing cellular proliferation. Chitooligosaccharide (COS)–carboxymethyl chitosan (CMC)–polyethylene glycol diacrylate (PEGDA) hydrogels with vancomycin were evaluated to ascertain their minimum inhibitory concentration (MIC) and minimum bactericidal concentration (MBC) values (Fig. S2, ESI†). The MIC was determined as the concentration of the test substance necessary to inhibit the color change from blue to pink, signifying bacterial presence. Our findings demonstrated the efficacy of the vancomycin-encapsulated COS–CMC–PEGDA hydrogel against *K. pneumoniae* ATCC 13883. These hydrogels exhibited a broad minimum inhibitory concentration, ranging from 10 mg mL^{-1} to 0.0195 mg mL^{-1}. The MIC was determined to be 5 mg mL^{-1} for *N*(D) and 2.5 mg mL^{-1} for 4°(D), while it was 2.5 mg mL^{-1} for vancomycin hydrochloride (Table S2, ESI†). These values were cross-checked by the MBC test. This study utilized this cutoff to assess the antibacterial efficacy of vancomycin-encapsulated COS–CMC–PEGDA hydrogel and the proportion of viable bacteria (live/dead cells). 4°(D) showed the same result as the drug when used directly, indicating superior drug release and incorporation over *N*(D).

Table 2 Zones of inhibition for the well diffusion and disc diffusion assay against a Gram-negative bacterium (*K. pneumoniae* ATCC 13883) and a Gram-positive bacterium (*B. cereus* ATCC 14579)

		Zone of inhibition (mm) (mean ± SD)			
		B. cereus		*K. pneumoniae*	
	Concentration (mg mL^{-1})	Well diffusion	Disc diffusion	Well diffusion	Disc diffusion
N (D)	10	26 ± 0.625	19 ± 0.675	0	0
4° (D)		29 ± 0.115	22 ± 0.225	14 ± 0.85	0
Vancomycin ($^{+Ve}$C)		31 ± 0.75	25 ± 0.950	16 ± 0.9	10 ± 0.75

4. Conclusion

Chitooligosaccharide (MW = 12.8 kDa, DD = 62.5%) was used to form a chitooligosaccharide (COS)–carboxymethyl chitosan (CMC)–polyethylene glycol diacrylate (PEGDA) hydrogel through UV crosslinking. Vancomycin hydrochloride was incorporated, and its drug release kinetics were studied under different conditions. The FTIR and XRD analyses confirm the incorporation of vancomycin into the hydrogels. The DSC–TGA results further confirmed that the interaction and showed degradation at temperature ranges of 280–300 °C and 380–400 °C, owing to breakage of cyclic bonds and amide, ether linkages, respectively. The swelling behavior was explained using the LCST behavior of the hydrogels under different conditions. A mechanism of interaction was postulated between vancomycin and the hydrogels, and the effect of this changing interaction was used to analyze swelling behavior and drug release patterns. The polyelectrolyte complex (PEC) nature of the hydrogel helped to achieve pH and temperature-sensitive release. *N*(D)-Regular hydrogel at 1.2 pH showed higher drug release than at 6.8 pH. 4°(D) showed no distinct pattern for drug release, with the highest release (98%) for 6.8 pH at 37 °C. The drug release data were fitted into the different mathematical models, with the Korsmeyer–Peppas model fitting the data most accurately on most occasions. 4°(D) hydrogel exhibited a greater inhibitory effect against Gram-positive bacteria *B. cereus* compared to *N*(D). Also, it showed a lower minimum inhibitory concentration (MIC) and minimum bactericidal concentration (MBC) compared to *N*(D).

In most conditions, 4°(D) hydrogel showed a higher drug release (%) compared to *N*(D) with a *p*-value <0.05. Also, the better incorporation of the drug in the case of 4°(D) and superior antibacterial activity against Gram-positive bacteria leads to the conclusion that 4°(D) hydrogel is a better drug delivery system compared to *N*(D). 4°(D) hydrogel is a better choice for colonic applications. These findings indicate that antibiotics like vancomycin can be incorporated in 4°(WD) to combat infections caused by other Gram-positive bacteria such as *Staphylococcus aureus*, *S. epidermidis*, *S. pyogenes*, *S. pneumoniae*, *Streptococcus viridans*, and species of *Bacillus*, *Actinomyces*, *Clostridium*, and *Corynebacterium*.[32] Although this study has proposed a temperature-dependent formulation of polysaccharide-based hydrogel for a pH/temperature sensitive targeted colonic delivery of an antibiotic, this method can be used to explore the targeted drug delivery to the colon for common colonic diseases such as ulcerative colitis, Crohn's disease, colorectal cancer, constipation, spastic colon, and irritable bowel syndrome.

This work establishes the potential of biomixing temperature in developing better drug delivery systems. The biomixing temperature can be altered for better efficacy against Gram-positive bacteria such as *S. epidermidis*, *S. pyogenes*, *S. pneumoniae*, *S. viridans*, *etc.*, and for the treatment of various colonic diseases. For future work, other biomixing temperatures besides 4 °C can be investigated to develop a more comprehensive understanding of the parameter's potential in designing more effective DDSs. Moreover, *in vivo* studies involving rabbits or mice to corroborate the efficacy of such DDSs can also be explored.

Author contributions

Mohammad Muhtasim Ittisaf: conceptualization, methodology, data curation, formal analysis, investigation, validation, visualization, writing – original draft, writing – review; Rakid-Ul-Haque: methodology, data curation, formal analysis, investigation, validation, visualization; Nishat Tabassum: investigation, writing – review; Mehedi Hasan Pritom: investigation, writing – original draft; Md. Shad Hossain Tanvir: investigation, writing – review; M. Azam Ali: conceptualization, methodology, resources, writing – review & editing, supervision Shoeb Ahmed: conceptualization, methodology, resources, writing – review & editing, supervision, project administration.

Data availability

Data for this article, including raw experimental readings and FTIR data are available from the Open Science Framework at Ahmed, S. 2024. ''COS Hydrogel pH/Temp Sensitive'' (OSF, 2024) (see <osf.io/2t7hr>).

Conflicts of interest

There are no conflicts to declare.

Acknowledgements

The authors acknowledge financial support from the Basic Research Grant from BUET and wish to thank the Applied Bioengineering Research Incubator (ABRI), BUET, the Institute of Food and Radiation Biology, Atomic Energy Commission, Savar for conducting gamma irradiation, and providing the facilities for the characterization studies.

References

1 A. Vashist, A. Vashist, Y. K. Gupta and S. Ahmad, Recent advances in hydrogel based drug delivery systems for the human body, *J. Mater. Chem. B*, 2014, **2**, 147–166.
2 Y. Tang, C. L. Heaysman, S. Willis and A. L. Lewis, Physical hydrogels with self-assembled nanostructures as drug delivery systems, *Expert Opin. Drug Delivery*, 2011, **8**, 1141–1159.
3 A. S. Hoffman, Hydrogels for biomedical applications, *Adv. Drug Delivery Rev.*, 2002, **54**, 3–12.
4 F. Shabir, *et al.*, Preparation and characterization of pH sensitive crosslinked Linseed polysaccharides-*co*-acrylic acid/methacrylic acid hydrogels for controlled delivery of ketoprofen, *Des. Monomers Polym.*, 2017, **20**, 485–495.
5 L. S. Tan, *et al.*, Fabrication of radiation cross-linked diclofenac sodium loaded carboxymethyl sago pulp/chitosan hydrogel for enteric and sustained drug delivery, *Carbohydr. Polym. Technol. Appl.*, 2021, **2**, 100084.
6 S. Das and U. Subuddhi, Controlled delivery of ibuprofen from poly(vinyl alcohol)–poly(ethylene glycol) interpenetrating polymeric network hydrogels, *J. Pharm. Anal.*, 2019, **9**, 108–116.
7 C. T. Gustafson, *et al.*, Controlled Delivery of Vancomycin via Charged Hydrogels, *PLoS One*, 2016, **11**, e0146401.
8 A. K. Jha, *et al.*, Molecular weight and concentration of heparin in hyaluronic acid-based matrices modulates growth factor retention kinetics and stem cell fate, *J. Controlled Release*, 2015, **209**, 308–316.
9 G. Lin, L. Cosimbescu, N. J. Karin and B. J. Tarasevich, Injectable and thermosensitive PLGA-g-PEG hydrogels containing hydroxyapatite: preparation, characterization and in vitro release behavior, *Biomed. Mater.*, 2012, **7**, 024107.
10 B. Chen, B. Wright, R. Sahoo and C. J. Connon, A Novel Alternative to Cryopreservation for the Short-Term Storage of Stem Cells for Use in Cell Therapy Using Alginate Encapsulation, *Tissue Eng. Part C Methods*, 2013, **19**, 568–576.
11 D. J. Menzies, *et al.*, Tailorable Cell Culture Platforms from Enzymatically Cross-Linked Multifunctional Poly(ethylene glycol)-Based Hydrogels, *Biomacromolecules*, 2013, **14**, 413–423.
12 P. A. McCarron, *et al.*, Preliminary clinical assessment of polyvinyl alcohol-tetrahydroxyborate hydrogels as potential topical formulations for local anesthesia of lacerations, *Acad. Emerg. Med.*, 2011, **18**, 333–339.
13 E. E. Coates, C. N. Riggin and J. P. Fisher, Photocrosslinked alginate with hyaluronic acid hydrogels as vehicles for mesenchymal stem cell encapsulation and chondrogenesis, *J. Biomed. Mater. Res. A*, 2013, **101A**, 1962–1970.
14 C. A. Brunner and R. W. Gröner, Carboxy-Methyl-Cellulose Hydrogel-Filled Breast Implants – An Ideal Alternative? a Report of Five Years' Experience with This Device, *Can. J. Plast. Surg.*, 2006, **14**, 151–154.
15 C. Muanprasat and V. Chatsudthipong, Chitosan oligosaccharide: Biological activities and potential therapeutic applications, *Pharmacol. Ther.*, 2017, **170**, 80–97.
16 S. Naqvi and B. M. Moerschbacher, The cell factory approach toward biotechnological production of high-value chitosan oligomers and their derivatives: an update, *Crit. Rev. Biotechnol.*, 2017, **37**, 11–25.
17 N. Tabassum, S. Ahmed and M. Azam Ali, Chitooligosaccharides for Drug Delivery, in *Chitooligosaccharides*, ed. S.-K. Kim, Springer International Publishing, Cham, 2022, pp. 309–332, DOI: 10.1007/978-3-030-92806-3_19.
18 P.-J. Park, J.-Y. Je and S.-K. Kim, Free Radical Scavenging Activity of Chitooligosaccharides by Electron Spin Resonance Spectrometry, *J. Agric. Food Chem.*, 2003, **51**, 4624–4627.
19 Y. Zheng, *et al.*, Protective effect of chitosan oligosaccharide against oxidative damage of peripheral blood mononuclear cells in dairy cows induced by diethylenetriamine/nitric oxide via NF-κB signalling pathway, *Ital. J. Anim. Sci.*, 2020, **19**, 602–609.
20 S. R. G. Sandri, M. C. Bonferoni, F. Ferrari, M. Mori and C. Caramella, The role of chitosan as a mucoadhesive agent in mucosal drug delivery, *J. Drug Deliv. Sci. Technol.*, 2012, **22**, 275–284.
21 M. Thanou, B. I. Florea, M. Geldof, H. E. Junginger and G. Borchard, Quaternized chitosan oligomers as novel gene delivery vectors in epithelial cell lines, *Biomaterials*, 2002, **23**, 153–159.
22 N. G. M. Schipper, *et al.*, Chitosans as absorption enhancers for poorly absorbable drugs 2: mechanism of absorption enhancement, *Pharm. Res.*, 1997, **14**, 923–929.
23 H.-C. Yang and M.-H. Hon, The effect of the molecular weight of chitosan nanoparticles and its application on drug delivery, *Microchem. J.*, 2009, **92**, 87–91.
24 M. Köping-Höggård, *et al.*, Chitosan as a nonviral gene delivery system. Structure–property relationships and characteristics compared with polyethylenimine in vitro and after lung administration in vivo, *Gene Ther.*, 2001, **8**, 1108–1121.
25 M. S. Rehmann, *et al.*, Tuning and Predicting Mesh Size and Protein Release from Step Growth Hydrogels, *Biomacromolecules*, 2017, **18**, 3131–3142.
26 H. Onishi and Y. Machida, Biodegradation and distribution of water-soluble chitosan in mice, *Biomaterials*, 1999, **20**, 175–182.
27 D. W. Lee, *et al.*, Effect of γ-Irradiation on Degradation of Alginate, *J. Agric. Food Chem.*, 2003, **51**, 4819–4823.
28 Z. Yuan, *et al.*, Enhanced accumulation of low-molecular-weight chitosan in kidneys: a study on the influence of N-acetylation of chitosan on the renal targeting, *J. Drug Target*, 2011, **19**, 540–551.
29 Y. Luo and Q. Wang, Recent development of chitosan-based polyelectrolyte complexes with natural polysaccharides for drug delivery, *Int. J. Biol. Macromol.*, 2014, **64**, 353–367.
30 T. Wu, Y. Li and D. S. Lee, Chitosan-based composite hydrogels for biomedical applications, *Macromol. Res.*, 2017, **25**, 480–488.
31 I. M. El-Sherbiny, E. M. Abdel-Bary and D. R. K. Harding, Swelling characteristics and in vitro drug release study with

pH- and thermally sensitive hydrogels based on modified chitosan, *J. Appl. Polym. Sci.*, 2006, **102**, 977–985.
32 F. R. Bruniera, *et al.*, The use of vancomycin with its therapeutic and adverse effects: a review, *Eur. Rev. Med. Pharmacol. Sci.*, 2015, **19**(4), 694–700.
33 A. Berthod, H. X. Qiu, S. M. Staroverov, M. A. Kuznestov and D. W. Armstrong, Chiral Recognition with Macrocyclic Glycopeptides: Mechanisms and Applications, in *Chiral Recognition in Separation Methods*, ed. A. Berthod, Springer Berlin Heidelberg, Berlin, Heidelberg, 2010, pp. 203–222, DOI: 10.1007/978-3-642-12445-7_7.
34 B. Tian and J. Liu, Smart stimuli-responsive chitosan hydrogel for drug delivery: A review, *Int. J. Biol. Macromol.*, 2023, **235**, 123902.
35 Z. M. Abid Al-Wahaab and M. H. Al-Mayahy, Microneedles as a potential platform for improving antibiotic delivery to bacterial infections, *Heliyon*, 2024, **10**, e37173.
36 S. Mantha, *et al.*, Smart Hydrogels in Tissue Engineering and Regenerative Medicine, *Materials*, 2019, **12**, 3323.
37 N. Tabassum, S. Ahmed and M. M. Ittisaf, Rakid-Ul-Haque, Md. & Ali, M. A. A green approach for depolymerization of chitosan: applications in hydrogels, *Cellulose*, 2023, **30**, 8769–8787.
38 M. Hakim Khalili, *et al.*, Additive Manufacturing and Physicomechanical Characteristics of PEGDA Hydrogels: Recent Advances and Perspective for Tissue Engineering, *Polymers*, 2023, **15**, 2341.
39 S. Alven and B. A. Aderibigbe, Chitosan and Cellulose-Based Hydrogels for Wound Management, *Int. J. Mol. Sci.*, 2020, **21**, 9656.
40 W. Tomal and J. Ortyl, Water-Soluble Photoinitiators in Biomedical Applications, *Polymers*, 2020, **12**, 1073.
41 T. Ur-Rehman, S. Tavelin and G. Gröbner, Effect of DMSO on micellization, gelation and drug release profile of Poloxamer 407, *Int. J. Pharm.*, 2010, **394**, 92–98.
42 M. Khaleghi, E. Ahmadi, M. Khodabandeh Shahraki, F. Aliakbari and D. Morshedi, Temperature-dependent formulation of a hydrogel based on Hyaluronic acid-polydimethylsiloxane for biomedical applications, *Heliyon*, 2020, **6**, e03494.
43 M. Khandaker, A. Orock, S. Tarantini, J. White and O. Yasar, Biomechanical Performances of Networked Polyethylene Glycol Diacrylate: Effect of Photoinitiator Concentration, Temperature, and Incubation Time, *Int. J. Biomater.*, 2016, **2016**, 1–8.
44 Y. Setiyorini, X. Lou and S. Pintowantoro, The Influence of Temperature and Drug Concentrations Prednisolone in NIPAAm Copolymer, *Procedia Chem.*, 2012, **4**, 336–342.
45 X. Zhu, *et al.*, Tuning complexation of carboxymethyl cellulose/cationic chitosan to stabilize Pickering emulsion for curcumin encapsulation, *Food Hydrocolloids*, 2021, **110**, 106135.
46 S. Kaihara, Y. Suzuki and K. Fujimoto, In situ synthesis of polysaccharide nanoparticles via polyion complex of carboxymethyl cellulose and chitosan, *Colloids Surf., B*, 2011, **85**, 343–348.
47 P. Raut, S. Li, Y.-M. Chen, Y. Zhu and S. C. Jana, Strong and Flexible Composite Solid Polymer Electrolyte Membranes for Li-Ion Batteries, *ACS Omega*, 2019, **4**, 18203–18209.
48 J. Vazquez-Armendariz, *et al.*, Influence of Controlled Cooling on Crystallinity of Poly(L-Lactic Acid) Scaffolds after Hydrolytic Degradation, *Materials*, 2020, **13**, 2943.
49 G. Wypych, Analytical Methods, in *PVC Degradation and Stabilization*, Elsevier, 2015, pp. 241–285, DOI: 10.1016/B978-1-895198-85-0.50012-1.
50 M. Jurak, A. E. Wiącek, K. Przykaza, A. Ładniak and K. Woźniak, Temperature-dependent interactions in the chitosan/cyclosporine A system at liquid–air interface, *J. Therm. Anal. Calorim.*, 2019, **138**, 4513–4521.
51 N. Alemdar, Synthesis of chitosan-based hydrogel by using photopolymerization technique, *Anadolu Univ. J. Sci. Technol. - Appl. Sci. Eng.*, 2016, **17**, 391–400.
52 A. Vashist, *et al.*, Impact of Nanoclay on the pH-Responsiveness and Biodegradable Behavior of Biopolymer-Based Nanocomposite Hydrogels, *Gels*, 2019, **5**, 44.
53 T. López-León, E. L. S. Carvalho, B. Seijo, J. L. Ortega-Vinuesa and D. Bastos-González, Physicochemical characterization of chitosan nanoparticles: electrokinetic and stability behavior, *J. Colloid Interface Sci.*, 2005, **283**, 344–351.
54 Q. Z. Wang, *et al.*, Protonation constants of chitosan with different molecular weight and degree of deacetylation, *Carbohydr. Polym.*, 2006, **65**, 194–201.
55 H. Kono and T. Teshirogi, Cyclodextrin-grafted chitosan hydrogels for controlled drug delivery, *Int. J. Biol. Macromol.*, 2015, **72**, 299–308.
56 K.-L. Deng, *et al.*, Drug release behaviors of a pH/temperature sensitive core-shelled bead with alginate and poly(N-acryloyl glycinates), *Front. Mater. Sci. China*, 2010, **4**, 353–358.
57 N. Dhar, S. P. Akhlaghi and K. C. Tam, Biodegradable and biocompatible polyampholyte microgels derived from chitosan, carboxymethyl cellulose and modified methyl cellulose, *Carbohydr. Polym.*, 2012, **87**, 101–109.
58 K. Son and J. Lee, Synthesis and Characterization of Poly(Ethylene Glycol) Based Thermo-Responsive Hydrogels for Cell Sheet Engineering, *Materials*, 2016, **9**, 854.
59 Y. Pei, *et al.*, The effect of pH on the LCST of poly(N-isopropylacrylamide) and poly(N-isopropylacrylamide-*co*-acrylic acid), *J. Biomater. Sci. Polym. Ed.*, 2004, **15**, 585–594.
60 J. S. Claudius and S. H. Neau, The solution stability of vancomycin in the presence and absence of sodium carboxymethyl starch, *Int. J. Pharm.*, 1998, **168**, 41–48.
61 T.-Y. Liu, S.-Y. Chen, Y.-L. Lin and D.-M. Liu, Synthesis and characterization of amphiphatic carboxymethyl-hexanoyl chitosan hydrogel: water-retention ability and drug encapsulation, *Langmuir*, 2006, **22**, 9740–9745.
62 H. Namazi and A. Kanani, Investigation diffusion mechanism of β-lactam conjugated telechelic polymers of PEG and β-cyclodextrin as the new nanosized drug carrier devices, *Carbohydr. Polym.*, 2009, **76**, 46–50.
63 Mathematical models of drug release, in *Strategies to Modify the Drug Release from Pharmaceutical Systems*, ed. M. L. Bruschi, Elsevier, 2015, ch. 5, pp. 63–86.

64 E. Van Groesen, *et al.*, Vancomyxins: Vancomycin-Polymyxin Nonapeptide Conjugates That Retain Anti-Gram-positive Activity with Enhanced Potency against Gram-negative Strains, *ACS Infect. Dis.*, 2021, **7**, 2746–2754.
65 R. Nagarajan, Antibacterial activities and modes of action of vancomycin and related glycopeptides, *Antimicrob. Agents Chemother.*, 1991, **35**, 605–609.
66 D. M. Livermore, Antibiotic uptake and transport by bacteria, *Scand. J. Infect. Dis. Suppl.*, 1990, **74**, 15–22.